Uncertainties in the dielectric constant model for seawater in FASTEM and implications for the cal/val of new microwave instruments

Heather Lawrence, Niels Bormann, Alan Geer, Stephen English

ECMWF, Shinfield Park, Reading, RG2 9AX, United Kingdom

1 INTRODUCTION

In the GAIA-CLIM H2020 project, the lack of accurate uncertainty estimates for the FASTEM ocean emissivity model has been identified as a gap in our ability to perform satellite cal/val to reference standards. This particularly affects microwave imagers (considered in this study) but also has implications for surface-sensitive microwave sounding channels. As a first step in the estimation of this uncertainty, we consider the contribution from the dielectric constant term by comparison to laboratory measurements. Unfortunately, to-date no measurements have been taken with reference standard uncertainty estimates which follow the procedures set out by national measurement standards laboratories. There are, however, a number of measurements taken with stated uncertainties. In this paper we compare FASTEM to a range of measurements for the dielectric constant in brightness temperature space. We use atmospheric and surface variables from the ECMWF forecasts to transform both the dielectric constant measurements and model values into brightness temperatures at the frequencies of microwave imagers, and compare these values. The measurement uncertainties are also transformed into brightness temperature space. We further examine the O - B statistics of GMI and AMSR-2 to evaluate whether there are skin-temperature dependent biases which could indicate errors in the FASTEM dielectric constant model for seawater.

2 Top of the atmosphere brightness temperatures for the surface-sensitive channels of microwave sounding and imaging instruments

The Top of the Atmosphere (TOA) brightness temperature (T_B) of microwave imagers and sounders can be expressed as a summation of three terms, including (1) the ocean (or land) surface emission, attenuated by the atmosphere, (2) the upward atmospheric emission, and (3) the downward emission, which is partially reflected upwards by the surface, and then attenuated by the atmosphere. Mathematically this can be expressed as follows:

$$T_B = eT_s\Gamma + T_{down}\left(1-e\right)\Gamma + T_{up}, \tag{1}$$

where e is the emissivity, T_s the ocean skin temperature, Γ is the surface-to-space transmittance, and T_{up} and T_{down} are respectively the upward and downward emission terms. Note that T_{down} includes both the downward emission of the atmosphere and the cosmic microwave background radiation at-

tenuated by the atmosphere. For all channels of microwave imagers, and the surface-sensitive channels of sounders, Γ is non-zero, such that the surface contribution to the top of the atmosphere brightness temperature is non-negligible. For humidity-sensitive channels of microwave imagers, in dry atmospheres the value of Γ approaches 1 for many channels and the surface contribution becomes the main component.

For a flat ocean surface, the ocean emissivity can be calculated as a function of the dielectric constant (permittivity) of seawater using the standard Fresnel equations (which are themselves derived from Maxwell's equations). However, surface riples and large-scale waves as well as foam coverage increase the ocean surface emissivity so that the Fresnel equations are no longer valid. The FAST Emissivity Model (FASTEM) is used in RTTOV to account for these effects, expressing the emissivity as:

$$e = [1 - F(u_{10m})] \left[1 - R_0(\varepsilon, \theta) exp(-s_{cor}(u_{10m}, \nu) cos^2\theta) - R_{large}(u_{10m}, \theta)\right] + F(u_{10m}) \left[1 - R_{foam}(\theta, \nu)\right] + e_{wind\_direction}(u_{10m}, \phi), \quad (2)$$

where F is the foam fraction, R_0 is the Fresnel flat-surface reflectivity, s_{cor} is the small-scale correction in the reflectivity due to ripples on the ocean surface, R_{large} is the reduction in reflectivity due to large scale waves, R_{foam} is the reflectivity of the foam-covered surface, and $e_{wind\_direction}$ is the corrective term for the wind direction relative to the satellite azimuth angle. The V-polarisation and H-polarisation Fresnel reflectivities are expressed as the square of the magnitude of the (complex) reflection coefficients, $r_{0,V}$ and $r_{0,H}$, as follows:

$$R_{0,V} = |r_{0,V}|^2 = \left| \frac{\varepsilon(\nu) cos\theta - \sqrt{\varepsilon(\nu) - sin^2\theta}}{\varepsilon(\nu) cos\theta + \sqrt{\varepsilon(\nu) - sin^2\theta}} \right|^2 \quad (3)$$

$$R_{0,H} = |r_{0,H}|^2 = \left| \frac{cos\theta - \sqrt{\varepsilon(\nu) - sin^2\theta}}{cos\theta + \sqrt{\varepsilon(\nu) - sin^2\theta}} \right|^2 \quad (4)$$

In addition to the modification of the ocean emissivity in rough surface conditions, FASTEM also applies a modification factor to the $1 - e$ term in (1), representing the reflectivity of the surface. This is to account for non-anisotropic downwelling radiation which necessitates a correction for non-planar reflecting surfaces. The reflective term is a function of wind-speed and viewing angle, and with the addition of this term (1) is expressed as:

$$T_B = eT_s\Gamma + z(\nu, u_{10m}) T_{down} (1 - e) \Gamma + T_{up}, \quad (5)$$

where z is the downwelling correction term, dependent on frequency and wind-speed.

As indicated in the above equations, the FASTEM emissivity depends on the 10m wind-speed, u_{10m}, the satellite viewing angle, θ, the frequency, ν, the wind-direction relative to the satellite azimuth angle ϕ, and the complex dielectric constant of seawater, ε.

FASTEM was initially proposed by English and Hewison (1998) as an approximate method which is fast enough to be used in retrieval algorithms, and it has been developed and validated over a number of years. Currently version 6 is used in the RTTOV forward model at ECMWF and other NWP centres.

Bormann et al. (2012) summarise the main changes in the models from versions 1 - 5. The current version of FASTEM used at ECMWF (version 6) includes the foam cover parameterisation of Monahan and O'Muircheartaigh (1986), the downwelling correction term developed by Deblonde and English (2001), the dielectric constant model and the large scale and small scale wave terms developed by Liu et al. (2011), and the wind direction term developed by Kazumori and English (2015).

The dielectric constant of seawater, ε, is modelled in FASTEM as a function of temperature using the equations developed by Liu et al. (2011) and was included in FASTEM from version 4 onwards. In this paper we aim to evaluate the uncertainties in the dielectric constant terms predicted by the model of Liu et al. (2011), which we shall also refer to as FASTEM-4, and transform them into radiance space, as a first step in estimating the uncertainty of FASTEM for the calibration/validation of microwave imagers and sounders.

3 The Dielectric Constant of Seawater

The dielectric constant of a material is a measure of how it responds to an external electric field. When a time-varying electric field, such as an electromagnetic (EM) wave, is applied to a material, it becomes polarised. The degree of polarisation is determined by the dielectric constant, ε, and this will depend on the frequency, υ, of the EM wave. At microwave frequencies, the motions of particles in the presence of an electric field display relaxations. This means that there is a delay or lag in the polarisation of the material, due to the short-range interactions of the particles as they move in response to the field. This leads to a phase change between the applied electric field E and the resulting polarisation in the material. Due to the short-wave interactions, there is also a loss of energy as the EM wave passes through the material. Because of these two effects, the dielectric constant in the presence of a harmonic applied electric field (i.e. an EM wave) is expressed as a complex number:

$$\varepsilon(\upsilon) = \varepsilon'(\upsilon) + i\varepsilon''(\upsilon), \tag{6}$$

where each term is frequency-dependent. The real and imaginary terms of the square root of ε determine respectively the phase change, and the loss of electromagnetic energy dissipated in the material. In conductive media, the application of an electric field will also lead to a current, whose current density, j, depends on the conductivity of the medium, σ, and the applied electric field, E, as follows:

$$j = \sigma E. \tag{7}$$

To account for this effect, an additional (negative) imaginary term is added to (6) so that it becomes:

$$\varepsilon(\upsilon) = \varepsilon'(\upsilon) + i\varepsilon''(\upsilon) - i\frac{\sigma}{2\pi\varepsilon_0\upsilon}. \tag{8}$$

At low frequencies and in polar liquids the conductivity term dominates over the dielectric constant term of $\varepsilon''(\upsilon)$. For measurements of the dielectric constant the conductivity term is usually included in ε'' and we shall also adopt this convention.

The frequency-dependence of the dielectric constant for liquids can be modelled in the ideal case by the Debye dielectric model, which is given by:

$$\varepsilon(\upsilon) = \varepsilon(\infty) + \frac{\varepsilon(0) - \varepsilon(\infty)}{1 + i\omega\tau} - i\frac{\sigma}{2\pi\varepsilon_0\upsilon}. \tag{9}$$

This equation assumes that the dielectric constant varies between a high frequency value $\varepsilon(\infty)$ and the value for a static electric field $\varepsilon(0)$, with a relaxtion time of τ. If a static field were applied and then removed, the polarisation of the material would fall exponentially. τ is the time it would take for a material's polarisation to fall by 1/e from its maximum value.

The Debye equation has been shown to be a good approximation for the microwave dielectric constant of both pure water and seawater at lower frequencies (e.g. Kaatze and Uhlendorf (1981), Ellison et al. (1996a, 1998)). However at higher frequencies the form of (9) does not fit the experimental data (see e.g. Ellison et al. (2003)). In order to fit the measured dielectric constant of seawater at higher frequencies, the use of a 'double-Debye' model with two relaxation frequencies has been proposed by a number of authors (e.g. Stogryn et al. (1995), Ellison et al. (2003)). This follows on from theoretical suggestions of a second relaxation frequency for pure water (Haggis et al., 1952, Grant and Shepherd, 1974, Barthel et al., 1990) and experimental data indicating the presence of a second relaxation frequency for aqueous solutions (Barthel et al., 1992). However it is worth noting that while this fits the microwave data well, the high frequency value of $\varepsilon(\infty)$ derived from a double-Debye best-fit is not consistent with the high frequency measurements of the dielectric constant of water in the infra-red region. The double-Debye model should therefore be considered as somewhat empirical. The double-Debye model is expressed as:

$$\varepsilon(\upsilon) = \varepsilon(\infty) + \frac{\varepsilon(0) - \varepsilon_1}{1 + i\omega\tau_1} + \frac{\varepsilon_1 - \varepsilon(\infty)}{1 + i\omega\tau_2} - i\frac{\sigma}{2\pi\varepsilon_0\upsilon}, \tag{10}$$

for relaxation times τ_1 and τ_2 and an 'intermediate' dielectric constant value of ε_1. The terms $\varepsilon(\infty)$, $\varepsilon(0)$, ε_1, τ_1, τ_2 and the conductivity, σ, were found experimentally to vary as a function of temperature and (for low frequencies) salinity. However, as shown by Ellison et al. (1998), the salinity dependence of the dielectric constant reduces with increasing frequency, and is less than 3% above frequencies of around 37 GHz. The double-Debye model is used for the dielectric constant of seawater in FASTEM and other models, including the model of Meissner and Wentz (2004).

The double-Debye equation describes the frequency-dependence of ε, with the terms $\varepsilon(\infty)$, $\varepsilon(0)$, ε_1, τ_1, τ_2, σ derived empirically as a function of salinity and temperature using laboratory measurements. In the derivation of FASTEM-4, the double-Debye coefficients were fit to the dielectric constant measurements of Ho and Hall (1973), Ho et al. (1974), Ellison et al. (1998) and Ellison et al. (2003) for seawater and the dielectric constant measurements of Hasted et al. (1987), Lamkaouchi et al. (2003) and the pseudo measurements of Kaatze and Uhlendorf (1981) for pure water. These measurement sets cover a wide frequency range of 1.4 - 400 GHz. However, it is worth noting that there were no seawater measurements used in the frequency range of 3 - 20 GHz, where water measurements cannot be used as a substitute.

4 Measurements of the Dielectric constant of seawater in the literature

Most of the measurements of the dielectric constant of seawater available in the literature were carried out by Ellison and colleagues at the Physique des Interactions Ondes-Matiéres (PIOM) laboratory, at the university of Bordeaux, France, from 1996 to 2003 (Ellison et al., 1996a, 1998, 2003). These measurements were carried out using two different experimental set-ups. A Hewlett-Packard measuring system, described by Ellison et al. (1998), was used for measurements at frequencies in the range 3 - 20 GHz, and an ABmm measuring system as described by Lamkaouchi et al. (2003) was used for frequencies of 20 - 100 GHz. Lamkaouchi et al. (2003) estimated the measurement uncertainty of both set-ups by taking measurements of pure water and comparing the values obtained to those in the literature. They estimated their measurement uncertainties to be 1% for frequencies below 20 GHz and 3% for frequencies above. Measurements of the dielectric constant of seawater were also taken by Ho and Hall (1973) and Ho et al. (1974) at frequencies of 1.43 GHz and 2.65 GHz respectively, and using a resonant cavity method. These measurements have been used in the derivation of a number of different models including the Klein and Swift model (Klein and Swift, 1977) and FASTEM-4 (Liu et al., 2011), however they are not considered here since we concentrate on microwave imager frequencies.

While measurements of the dielectric constant of seawater are rather scarce, there is a large body of data available for the dielectric constant of pure water. Measurements taken up to 1996 which include uncertainty values have been usefully tabulated by Ellison et al. (1996b). These pure water measurements can be used in the derivation of the dielectric constant of seawater at higher frequencies, since the effect of the salinity has been shown to reduce with increasing frequency (Ellison et al., 1998). Indeed, both FASTEM-4 and the model of Meissner and Wentz (2004) were developed to be used for both freshwater and sea-water, with coefficients derived using a combination of measurements for both seawater and freshwater. The measurements for pure water date back to the 1940s, but the earlier measurements are likely subject to larger experimental errors due to less accurate measurement techniques. Stogryn et al. (1995) chose to exclude all experimental data from before 1970 in their double-Debye fit for pure water, for example. We note that most measurements for the dielectric constant of pure water tabulated by Ellison et al. (1996b) have measurement uncertainties of 1-3%.

The pure water measurements most commonly used for the derivation of dielectric constant models of freshwater and seawater, are those of Hasted et al. (1987) for high frequencies (176 - 410 GHz), and the pseudo data of Kaatze and Uhlendorf (1981). Hasted et al. (1987) do not state uncertainties for their measurements. Kaatze and Uhlendorf (1981) took measurements at frequencies up to 70 GHz, and supplemented these with values found in the literature to create a large dataset. The authors do not publish the measurements themselves but instead perform a single-Debye fit at spot temperatures and produce tables of the single-Debye parameters at these temperatures. For their own measurements, Kaatze and Uhlendorf (1981) publish a table of uncertainties in ε' and ε'' which vary with different frequency ranges (although they do not give information on how these were calculated). The uncertainties vary from 0.5 - 1.0% for frequencies up to 18 GHz, around 2% for frequencies from 18 - 30 GHz, 2 - 4% up to 40 GHz, and are 10% in ε' and 2.5% in ε'' for frequencies of 40-60 GHz. They also give uncertainties in the estimated values of ε_0, ε_∞ and τ for their single-Debye fit at different temperatures and frequencies. These transform into uncertainties in ε' of 0.2 - 2.0%, and uncertainties in ε'' of 0.006 - 0.7%. However they further compare their fit to measurements and state that the maximum measurement-model differences are 1% below 35 GHz and 5% above.

The measurements used in this study are indicated in Table 1. They include the experimental data used in the derivation of FASTEM-4 as well as some additional data. We concentrated on the frequency range

of microwave imagers, from 7 GHz up to 90 GHz. Microwave imagers have channels with frequencies of (approximately) 6.9 GHz, 7.3 GHz, 10.7 GHz, 19 GHz, 23 GHz, 37 GHz and 89 GHz. Note that the lowest frequency used at ECMWF is 19 GHz since the 7 GHz and 10 GHz imager channels are not assimilated, but observation minus background statistics are routinely calculated for all imager channels, and we include an assessment of these lower frequencies for completeness. Furthermore the 10 GHz channels are highly sensitive to rain over oceans so that it might be beneficial to assimilate these channels in the future.

For the comparison we used seawater data from Ellison et al. (1998) and Ellison et al. (2003), used in the derivation of FASTEM-4, as well as the measurements of Ellison et al. (1996a). The report of Ellison et al. (1996a) is no longer available online, but was kindly provided to us by Laurence Eymard from l'OCEAN laboratory. We also compared FASTEM-4 to the pseudo measurements of Kaatze and Uhlendorf (1981), which were also used in the derivation of FASTEM-4. We created these pseudo measurements using the single-Debye fits of Kaatze and Uhlendorf (1981) at frequencies and temperatures where their actual measurements make up the majority of data in the fit, and used the uncertainties given for these measurements. We supplemented the water measurements of Kaatze and Uhlendorf (1981), used in the FASTEM derivation, with those of Pottel et al. (1980), Kaatze (1989) and Richards and Sheppard (1991). These three measurement sets were chosen because they are relatively recent (taken after 1970), provide data at microwave imager frequencies, provide uncertainty estimates and cover a range of temperatures. Table 1 summarises all of the measurements used in the comparison to FASTEM-4, and their uncertainty values.

Table 1: Measurements compared to the FASTEM-4 dielectric constant model including the frequency (f), temperature (T), and Salinity (S) range of the measurements, the assigned uncertainties and whether they were used in the derivation of FASTEM-4.

Measurements	**f (GHz)**	**T (° C)**	**S (‰)**	**uncertainties**	**used in FASTEM-4?**
Ellison et al. (1996a)	6.8, 10.65, 18.7, 23.85, 36.5, 89	-2 - 30	23 - 39	1% for f <20 GHz, 3% else	no
Ellison et al. (1998)	23.85, 36.5, 89	-2 - 30	39	3%	yes
Ellison et al. (2003)	30 - 105	-2 - 30	35	3%	yes
Kaatze and Uhlendorf (1981) pseudo data	5	-4 - 30	0	0.5% in ε', 3.0% in ε''	yes
	10	-4 - 30	0	1.0% in ε', 0.9% in ε''	yes
	20	-4 - 30	0	1.8% in ε', 0.8% in ε''	yes
	30	-4 - 30	0	4.0% in ε', 2.0% in ε''	yes
	40, 50, 60	-4 - 30	0	10.0% in ε', 2.5% in ε''	yes
Richards and Sheppard (1991)	90	0 - 50	0	1.15 - 4.8% in ε', 0.6 - 5.7% in ε''	no
Kaatze (1989)	36.44	10, 15, 30	0	2.5% in ε', 2.0% in ε''	no
Pottel et al. (1980)	1.8 - 57.8	25	0	0.5 - 10% in ε', 0.9 - 4.0% in ε''	no

5 Transforming dielectric constant measurements and uncertainties into radiance space

In this study we compare dielectric constant measurements to the FASTEM model in brightness temperature space. To do so we first transformed the dielectric constant measurements and (FASTEM) model values into brightness temperature space at microwave imager frequencies and for typical atmospheric and surface conditions, using an approximate version of (5) as follows. For surface-sensitive channels, the atmosphere can be approximated to a homogeneous slab of temperature T_{atm}, such that the upward and downward atmospheric emission can both be expressed as $(1-\Gamma)T_{atm}$. We can further make the assumption that $T_{atm} = T_s$, which is a good approximation for surface sensitive observations. (5) then becomes:

$$T_B = eT_s\Gamma\left(1 - z(\nu, u_{10m})\right) - T_s\Gamma\left(1 - z(\nu, u_{10m})\right) + \Gamma^2 z(\nu, u_{10m})\left(T_c - T_s\right)(1 - e) + T_s, \qquad (11)$$

where T_c is the temperature of the cosmic microwave background radiation, equal to 2.73 K.

The dielectric constant measurements and model values were transformed into brightness temperatures using (11) with the emissivity calculated from the dielectric constant, using the FASTEM-6 wind-speed dependent equations, i.e. (2) - (4). The incidence angle was assumed to be 53° (as for microwave imagers) and the surface-to-space transmittance values (Γ) and 10m wind speeds (u_{10m}) were taken from the ECMWF background (short-range forecast) fields at AMSR-2 observation locations. This was done as follows. Firstly the AMSR-2 background values for a 12-hour period were filtered to select only values over ocean, at low wind speeds (< 7m/s) and after cloud-screening. For this we followed the same filtering procedure as for the satellite O - B values, described in the next section. Then, for each dielectric constant measurement, an ensemble of background Γ and u_{10m} values were selected for the AMSR-2 channel at the relevant frequency where the skin temperature lay between ± 2 K of the dielectric constant measurement temperature value. This provided us with representative values of u_{10m} and Γ for dielectric constant measurements taken at different frequencies and temperatures. Each dielectric constant measurement was then transformed into an ensemble of brightness temperatures using the selected values of Γ and u_{10m}. The equivalent FASTEM 4 dielectric constant model values were also transformed into brightness temperatures, and the difference then taken between the measurement and model values in brightness temperature space. The mean difference was then calculated for each dielectric constant measurement. Note that in our calculations we did not include the wind direction term of FASTEM 6 since the wind direction information was not readily available. However this should introduce a relatively small error in our calculation since we filter for high wind speeds.

We also transformed uncertainties in the dielectric constant into brightness temperature space, by differentiating (5) with respect to the real and imaginary terms of the dielectric constant and then applying the following (well-known) formula for combining these uncertainties into the total uncertainty in brightness temperatures, σ_{TB}, as follows:

$$\sigma_{TB}^2 = \left(\frac{\partial T_B}{\partial \varepsilon'}\sigma_{\varepsilon'}\right)^2 + \left(\frac{\partial T_B}{\partial \varepsilon''}\sigma_{\varepsilon''}\right)^2 \qquad (12)$$

To obtain the differentials in (12), we differentiated FASTEM analytically with respect to both ε' and ε''. Since R_0 depends on the square root of a complex number this differentiation is not trivial, and so we

do not give the full derivation here. We verified this analytical differentiation by comparison to numerical approximation methods, however. The uncertainties were transformed into brightness temperature space using the same model Γ and u_{10m} selected for the dielectric constant measurements, and then the mean brightness temperature H and V polarisation uncertainty calculated for each dielectric constant measurement.

Upon calculating (12), we found that the uncertainties in brightness temperature space are dominated by the imaginary term of the dielectric constant for frequencies above approximately 10 GHz. This is due to the differential $\frac{\partial T_B}{\partial \varepsilon''}$ increasing with frequency, and is illustrated in Fig. 1 which shows the absolute values of $\frac{\partial T_B}{\partial \varepsilon'}$ and $\frac{\partial T_B}{\partial \varepsilon''}$ as a function of frequency. Note that this figure shows the values calculated with the Fresnel emissivity, but they are similar for FASTEM emissivity calculations.

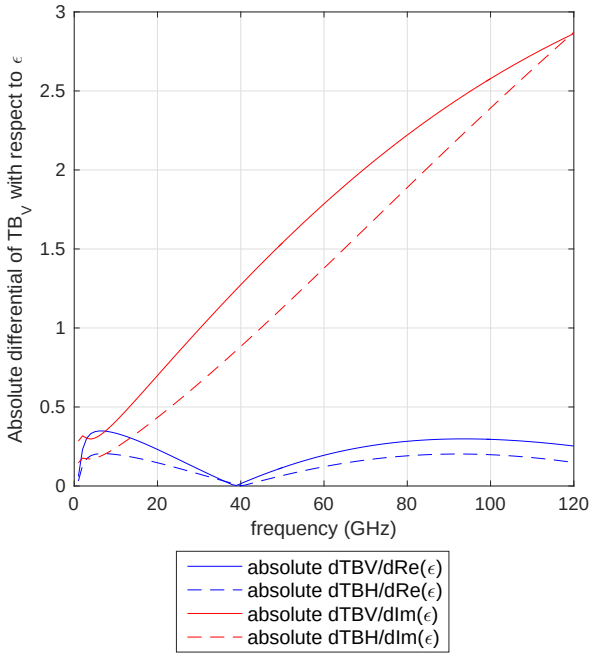

Figure 1: The absolute values of $\frac{\partial T_B}{\partial \varepsilon'}$ and $\frac{\partial T_B}{\partial \varepsilon''}$ for V and H polarisation, calculated for a temperature of 20°C, a salinity of 35‰, a viewing angle of 53°, surface-to-space transmittance of 1, and assuming Fresnel emissivity, shown as a function of frequency.

Most of the dielectric constant measurements for seawater and water have uncertainties that lie between 1 and 3%. When we transform these uncertainties into brightness temperatures they are of the order of 0.2 - 0.35 K and 0.6 - 1 K respectively (depending on the frequency). This is illustrated in Fig. 2 which shows the mean uncertainties for different imager channel frequencies, calculated for (a) a 1% uncertainty in the dielectric constant model values and (b) a 3% uncertainty in dielectric constant model values. Assuming there are no biases between FASTEM and the laboratory measurements, these values give us an estimate of the uncertainty in the dielectric constant model of FASTEM in brightness temperature space. However, these values may be an underestimation if there are disagreements between FASTEM and the measurements, as will be investigated in the next section.

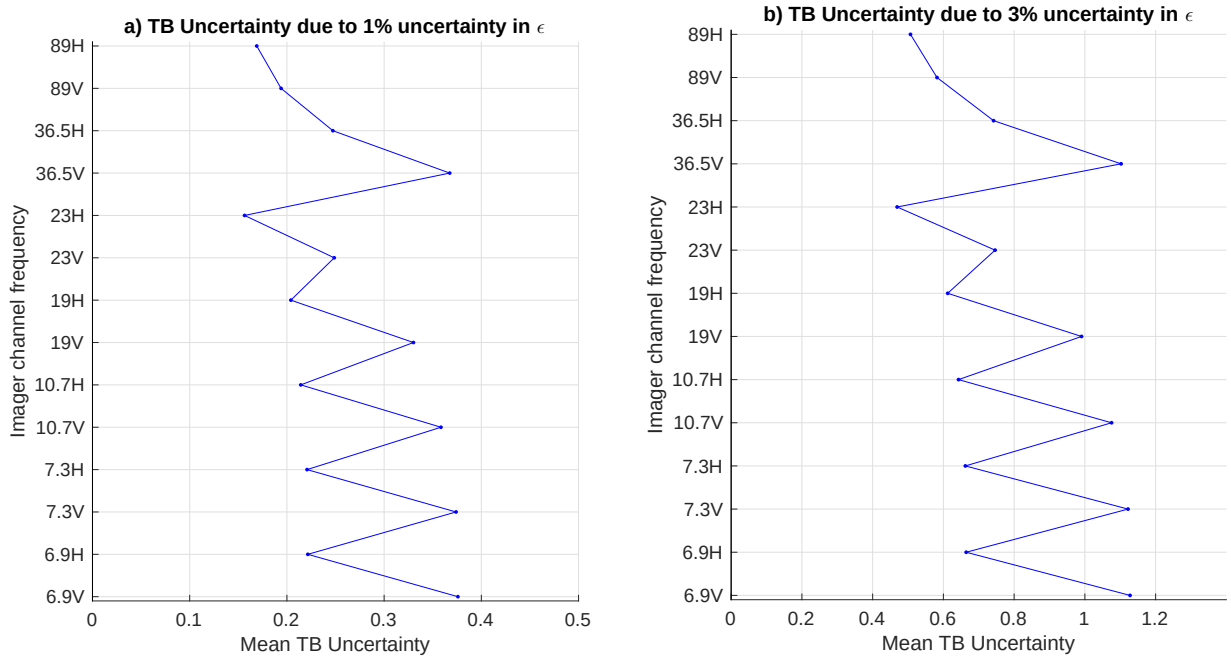

Figure 2: Uncertainty in brightness temperatures for microwave imager channels due to (a) 1% uncertainty in the dielectric constant model, and (b) a 3% uncertainty in the dielectric constant model. Values were calculated using the background model values of AMSR-2 in the ECMWF model, for a 12-hour period, and then the average uncertainty taken for each channel.

6 Results: Comparing FASTEM-4 and dielectric constant measurements in radiance space

The dielectric constant measurements minus FASTEM were calculated in radiance space as a function of (skin) temperature for different microwave imager frequencies. These were compared to O - B values for the AMSR-2 and GMI microwave imagers. These latter values were calculated using the ECMWF all-sky system. Mean O - B values were calculated using the ECMWF operational model background fields for the period 12 July 2017 - 31 December 2017 (cycle 43r3). Note that GMI version 5 data were used at ECMWF during this period. Background values were transformed into radiance space using RTTOV-SCATT version 11, which includes the effects of cloud and precipitation, and FASTEM version 6 (which uses the dielectric constant model of FASTEM version 4 with an assumed salinity of 35‰). The observations were superobbed before calculating O - B values, since this is done for operational assimilation. The data were additionally filtered for high wind speeds (keeping data with the 10m wind speed less than 7 m/s), with additional latitude, sea-ice and cloud filters. To filter for cloud, we made use of the cloud predictors C_{37}^{b} and C_{37}^{o}, which are used in the ECMWF assimilation system to calculate the observation error covariances. These predictors are based on respectively the first guess and observation brightness temperature differences for the 37 GHz V and H polarisation channels of AMSR-2 and GMI, as defined by Geer and Bauer (2010). The thresholds for all of the filters applied to the imager O - B values are given in Table 2.

Results of the dielectric constant measurements minus FASTEM in brightness temperature space are given in Figs. 3 - 8, as a function of (skin) temperature. The FASTEM dielectric constant values were calculated assuming the same salinity as the measurements for frequencies below 30 GHz, and with a

Table 2: Details of the calculation of O - B values for GMI and AMSR-2

Data filtering type	**Data selection criteria**
Cloud screening	$C_{37}^{b} < 0.05$ and $C_{37}^{o} < 0.05$
Cold-air outbreak screening	As developed by Lonitz and Geer (2015)
wind speed filtering	10m wind speed < 7 m/s
sea-ice screening	Model sea-ice fraction < 0.01 and -60° $<$ latitude $<$ 60°
land screening	Model land fraction < 0.01

constant salinity of 35‰ above 30 GHz (including for the water measurements) since the salinity has been found to have a negligible effect on the dielectric constant from frequencies at (approximately) 37 GHz and above (Ellison et al., 2003). Below 30 GHz we compare FASTEM to seawater measurements only, since pure water cannot be used as a proxy for seawater at these frequencies.

The results show that at frequencies of 7 - 24 GHz, there is disagreement between FASTEM and the dielectric constant measurements at low temperatures, and this disagreement lies outside of the measurement uncertainties. The laboratory measurements therefore indicate that there is a bias in FASTEM at these frequencies and at low temperatures.

In order to further evaluate whether there are biases in the FASTEM dielectric constant model we can also compare FASTEM to satellite data, by evaluating the mean observation minus background values of microwave imagers at different skin temperatures. When doing this one should bear in mind that statistics can also be affected by instrument calibration errors, particularly scene-temperature dependent errors, systematic errors in other aspects of the radiative transfer forward model, and/or systematic biases in the background fields. For example there could be residual cloud and/or undetected sea-ice.

The mean O - B values for GMI and AMSR-2 are shown in Fig.s 3 - 8 as a function of skin temperature. Note that the AMSR-2 statistics and the values at 6.8 GHz were not shown in the poster presented at ITSC-XXI. Also, the O - B statistics were calculated for a much longer period here - approximately 5 - 6 months (12 July - 31 December 2017), instead of 2 weeks as shown on the poster. As these plots show, there is a global bias difference of 2 - 4 K between AMSR-2 and GMI, indicating calibration and/or forward model errors for one or both of these instruments. For the purposes of this study, we therefore ignore the global average values and instead look at the relationship between mean O - B and the skin temperature. As previously noted, this could be affected by scene-temperature dependent biases for these instruments, which can occur if there are errors in the non-linearity corrections. However GMI has a 4-point calibration for the 10.7 - 36.5 GHz channels (see e.g. Wentz and Draper (2016)), making non-linearity errors unlikely for this instrument.

The mean O - B values for GMI and AMSR-2 show a positive bias at low skin temperatures at 6.8 and 10.65 GHz, relative to the O - B values at high skin temperatures, as shown in Figs. 3 and 4. The O - B gradients as a function of skin temperature rather support the hypothesis that FASTEM is biased at low temperatures, as the laboratory dielectric constant measurements would suggest. At 18.7 and 23.85 GHz there is also a slight gradient in O - B values at low temperatures, although at these frequencies the gradient is flatter than the gradient between the dielectric constant measurements and FASTEM. This indicates that there may be biases in FASTEM at these frequencies, but perhaps also

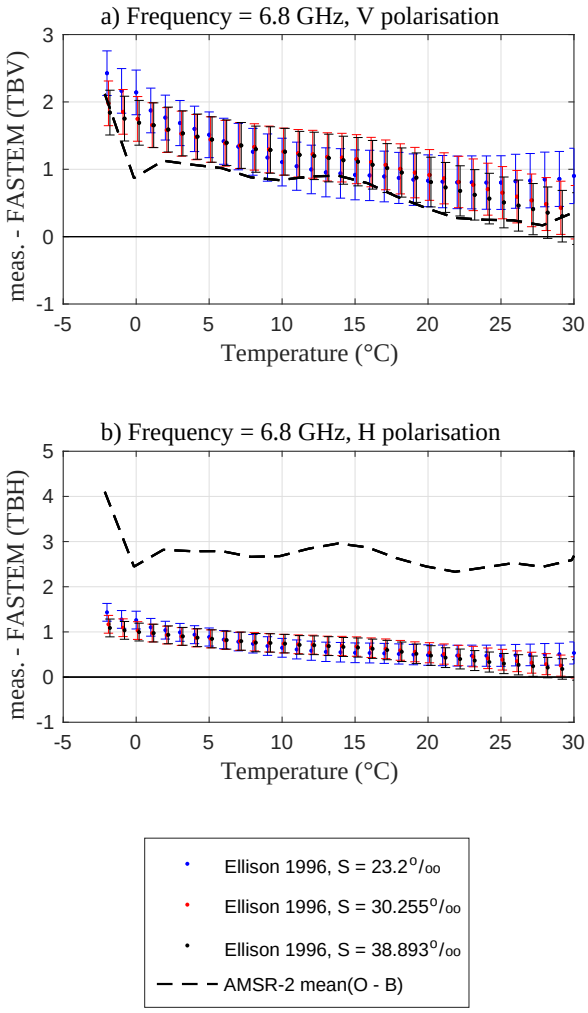

Figure 3: Dielectric constant measurements minus FASTEM-4 dielectric constant values, both transformed in radiance space for a frequency of 6.8 GHz and an angle of 53° for (a) V polarisation and (b) H polarisation, plotted as a function of temperature. Error bars show the dielectric constant measurement uncertainties also transformed into brightness temperatures. The FASTEM model brightness temperatures were calculated using the same salinity as the dielectric constant measurements. Microwave imager O - B values are also plotted.

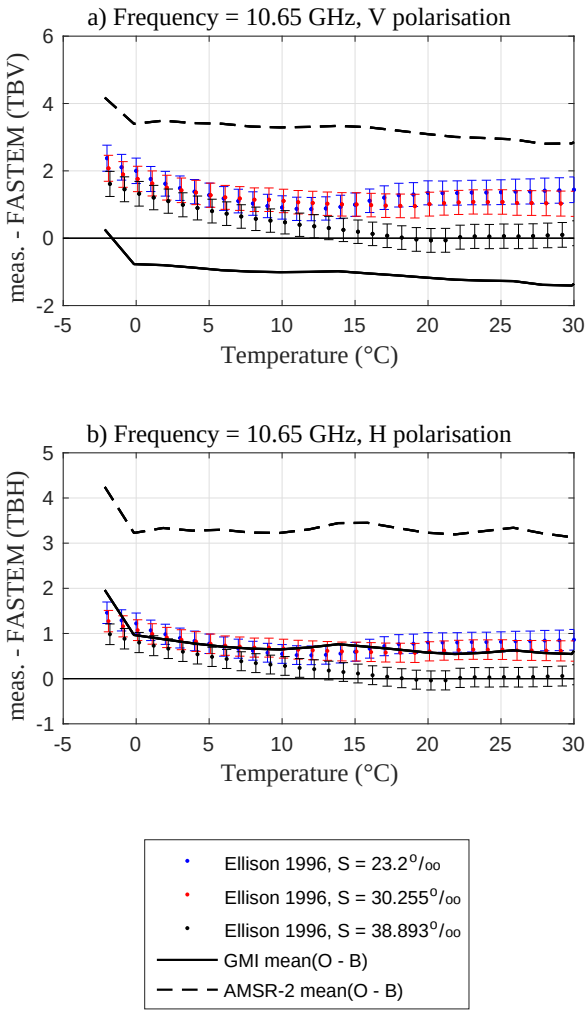

Figure 4: As Fig. 3 but for a frequency of 10.65 GHz.

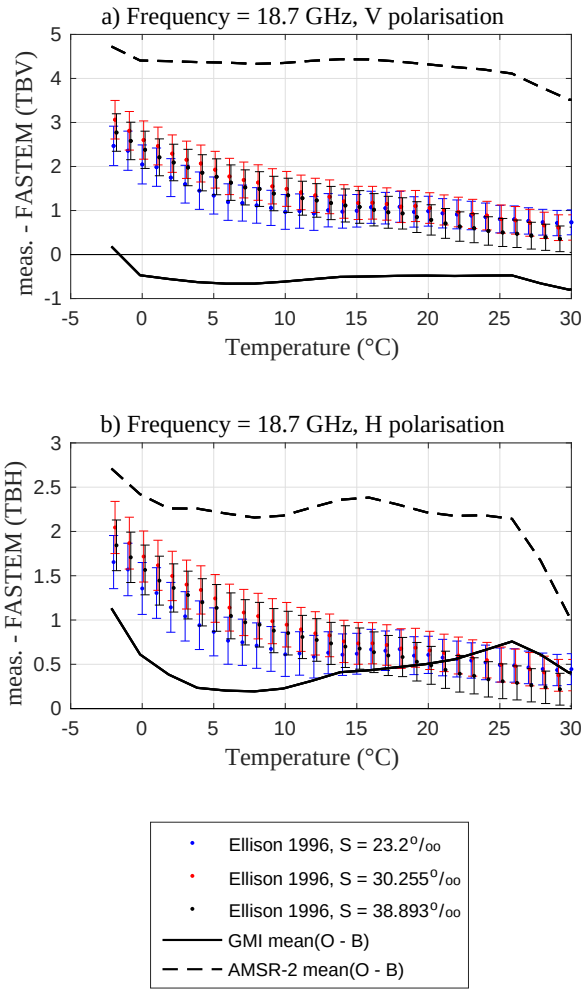

Figure 5: As Fig. 3 but for a frequency of 18.75 GHz.

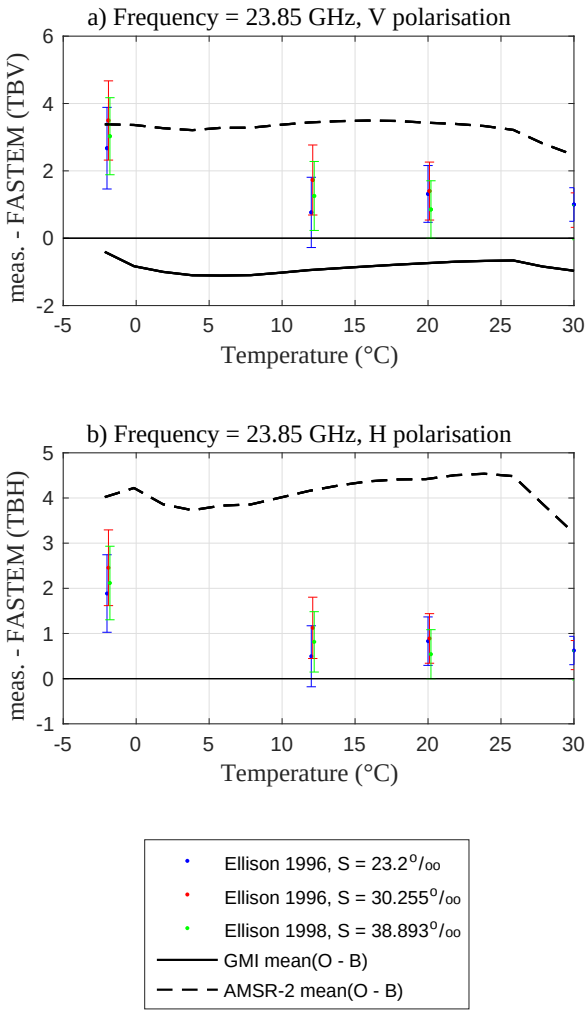

Figure 6: As Fig. 3 but for a frequency of 23.85 GHz.

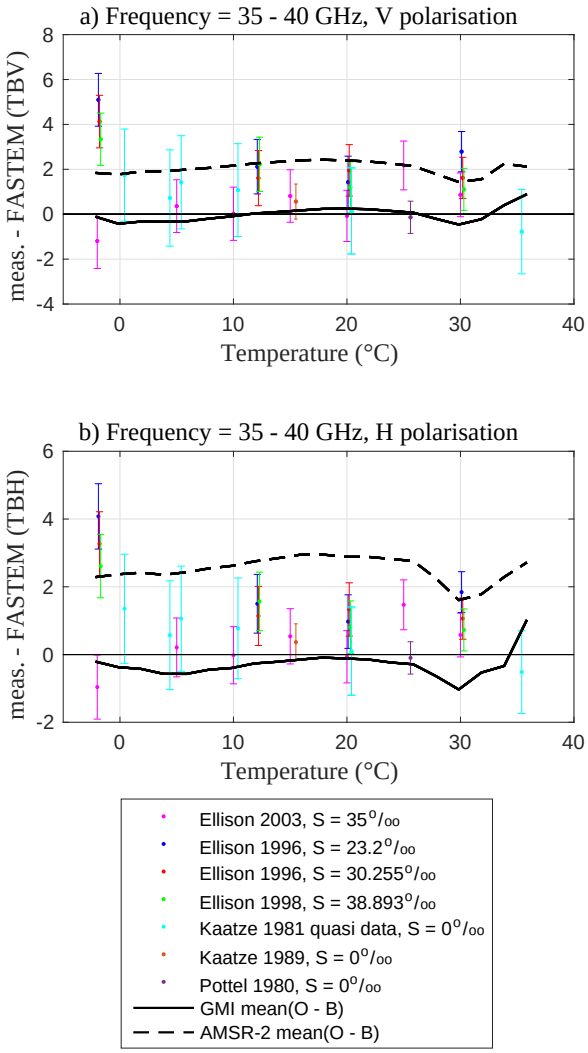

Figure 7: As Fig. 3 but for a frequencies of 35 - 37 GHz. Note that different measurements were taken at slightly different frequencies in this range. The FASTEM brightness temperatures were calculated assuming a salinity of 35‰.

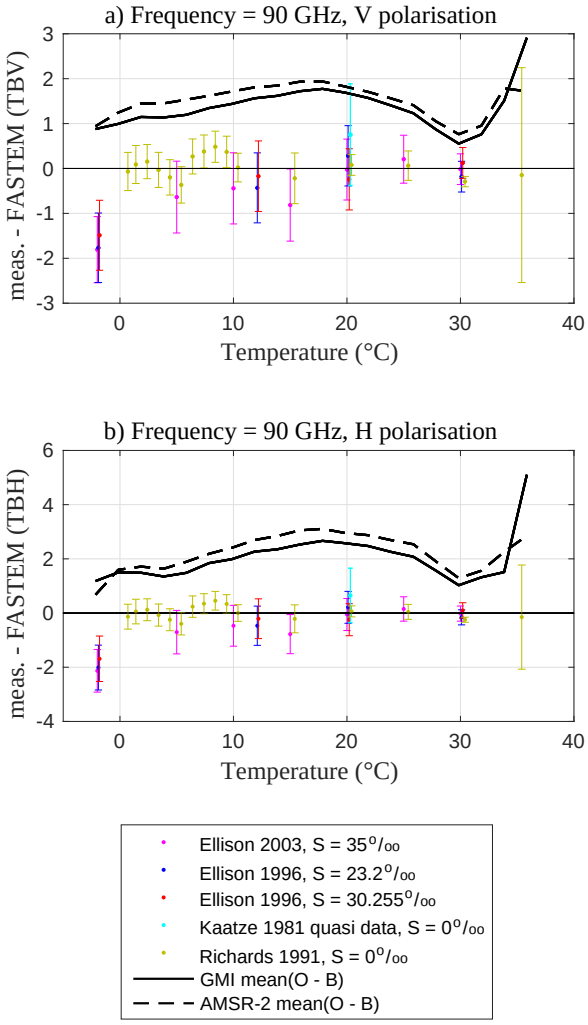

Figure 8: As Fig. 3 but for a frequencies of 89 - 90 GHz. Note that different measurements were taken at slightly different frequencies in this range. The FASTEM brightness temperatures were calculated assuming a salinity of 35‰.

errors in the dielectric constant measurements.

At 37 - 89 GHz there is no clear indication of a temperature-dependent bias in the FASTEM dielectric constant model, either in the comparison to dielectric constant measurements, or in the satellite O - B statistics. The exception is at -2°C where FASTEM does not agree with the measurements. At 35 - 40 GHz, there is also some disagreement between the different dielectric constant measurements, particularly at -2°C. This indicates that either there is an unknown systematic error in one of the measurement sets, or that the uncertainties are too low.

7 Conclusions

In this study we have evaluated the dielectric constant model used in FASTEM by comparison to laboratory measurements available in the literature which have associated measurement uncertainties. We performed this comparison in brightness temperature space at microwave imager frequencies, transforming also the measurement uncertainties into brightness temperature space. The comparison showed that there are disagreements between FASTEM and the measurements of Ellison et al. (1996a) at low temperatures and frequencies of 7 - 24 GHz, but that there is generally good agreement at frequencies of 37 and 89 GHz. The satellite O - B values for GMI and AMSR-2 also showed skin temperature dependent biases at low temperatures and lower frequencies (7 - 10 GHz), which could be a further indication of biases in the FASTEM dielectric constant model.

When transforming the dielectric constant measurements into radiance space we found that the brightness temperature uncertainties are dominated by the uncertainty in the imaginary part of the dielectric constant, for frequencies above around 10 GHz. Most measurements have uncertainties of 1 - 3 % in the dielectric constant, which translates to uncertainties of around 0.3 - 1 K. The lowest uncertainties were for the measurements of Richards and Sheppard (1991) at 89 GHz which were around 0.3 K in brightness temperature uncertainty. This provides us with an approximate estimate of the uncertainty in the FASTEM dielectric constant model for microwave imager frequencies of around 0.3 - 1 K. However, as previously stated, there are also biases of up to 2 K between FASTEM and the dielectric constant measurements at low frequencies and temperatures, and so the uncertainty should be higher in areas of cold ocean and for low frequency observations.

Given the biases observed between FASTEM and the measurements at 10 - 24 GHz, as well as some inconsistencies between different measurements at 37 GHz, it would be useful to have reference-quality traceable laboratory dielectric constant measurements of seawater (and/or pure water at higher frequencies) to be used to recalculate the FASTEM dielectric constant model. Traceable dielectric constant measurements have been taken for other polar liquids, such as by Gregory and Clarke (2009) for alcohols and at microwave frequencies up to 5 GHz, but not to our knowledge for seawater or pure water. Reference-quality measurements are needed for the full range of ocean temperatures as well as the frequencies for current and future microwave satellite instruments. Such measurements should include a comprehensive uncertainty analysis in which the uncertainty in each source of error is calculated, as well as identifying whether the error is systematic or random. It is important to also calculate the error correlations between the real and imaginary dielectric constant terms, since these measurements are usually not independent and such correlations should be taken into account either when transforming uncertainties into brightness temperatures or in deriving the FASTEM dielectric constant model terms. The measurement uncertainties should also be validated by intercomparison, preferably by comparing

to measurements taken using a different technique. Once reference quality measurements are available, the FASTEM dielectric constant model should be rederived, including with an estimation of the uncertainty. This is needed for performing cal/val of microwave surface-sensitive channels to reference standards.

Acknowledgements

Laurence Eymard is gratefully acknowledged for providing the report of Ellison et al. (1996a). The work of this poster was funded by the Horizon-2020 GAIA-CLIM project (grant 640276).

References

J. Barthel, K. Buchhuber, R. Buchner, and H. Hetzenauer. Dielectric spectra of some common solvents: Water and lower alcohols. *Chem. Phys. Lett.*, 165:369 – 373, 1990.

J. Barthel, H. Hetzenauer, and R. Buchner. Dielectric relaxation of aqueous electrolyte solutions. *Ber. Bunsenges. Phys. Chem.*, 96:988 – 997, 1992.

N. Bormann, A. Geer, and S. English. Evaluation of the microwave ocean surface emissivity mode FASTEM-5 in the IFS. *ECMWF tech. memo.*, 667, 2012.

G. Deblonde and S. J. English. Evaluation of the FASTEM 2 fast microwave oceanic surface emissivity model. *Tech. Proc. ITSC-XI Budapest*, pages 67 – 78, 2001.

W. Ellison, A. Balana, G. Delbos, K. Lamkaouchi, L. Eymard, C. Guillou, and C. Prigent. New permittivity measurements of seawater. *Radio Science*, 33(3):639–648, 1998.

W. J. Ellison, A. Balana, G. Delbos, K. Lamkaouchi, L. Eymard, C. Guillou, and C. Prigent. Study and measurement of the dielectric properties of sea water: Final report. *ESTEC/ESA contract*, 11197/94/NL/CN, 1996a.

W. J. Ellison, K. Lamkaouchi, and J.-M. Moreau. Water: a dielectric reference. *Journal of Molecular Liquids*, 68:171 – 279, 1996b.

W. J. Ellison, S. J. English, K. Lamkaouchi, A. Balana, E. Obligis, G. Deblonde, T. J. Hewison, P. Bauer, G. Kelly, and L. Eymard. A comparison of ocean emissivity models using the Advanced Microwave Sounding unit, the Special Sensor Microwave Imager, the TRMM Microwave Imager, and airborne radiometer observations. *Journal of Geophysical Research*, 108(D21), 2003.

S.J. English and T.J. Hewison. A fast generic microwave emissivity model. *In T. Hayasaka, D.L. Wu, Y. Jin, and J. Jiang (Eds.), Proceedings of SPIE, 3503*, pages 288 – 300, 1998.

A.J. Geer and P. Bauer. Enhaced use of all-sky microwave observations sensitive to water vapour, cloud and precipitation. *ECMWF Tech. Memo.*, 620, 2010.

E. H. Grant and R. J. Shepherd. Dielectric relaxation in water in the neighbourhood of 4C. *J. Chem. Phys.*, 60:1792 – 1796, 1974.

A. P. Gregory and R. N. Clarke. Traceable measurements of dielectric reference liquids over the temperature interval 10 - 50 c using coaxial-line methods. *Meas. Sci. Technol.*, 20, 2009.

G. H. Haggis, J. B. Hasted, and T. J. Buchanan. The dielectric properties of water in solutions. *J. Chem. Phys.*, 20:1452 – 1464, 1952.

J. B. Hasted, S. K. Husain, F. A. M. Frescura, and J. R. Birch. The temperature variation of the near millimeter wavelength optical constants of water. *Infr. Phys.*, 27:11 – 15, 1987.

W. Ho and W. F. Hall. Measurements of the dielectric properties of seawater and NaCl solutions at 2.65 GHz. *Journal of Geophys. Res.*, 78:6301 – 6315, 1973.

W. W. Ho, A. W. Love, and M. J. Van Melle. Measurements of the dielectric properties of sea water at 1.43 GHz. *NASA-CR-2458 report*, 1974.

U. Kaatze. Complex permittivity of water as a function of frequency and temperature. *J. Chem. Eng.*, 34:371 – 374, 1989.

U. Kaatze and V. Uhlendorf. The dielectric properties of water at microwave frequencies. *Z. Phys. Chem. Neue Folge*, 126:151–165, 1981.

M. Kazumori and S. English. Use of the ocean surface wind direction signal in microwave radiance assimilation. *Quart. J. Roy. Meteorol. Soc.*, 141:1354 – 1375, 2015.

L. A. Klein and C. T. Swift. An improved model for the dielectric constant of sea water at microwave frequencies. *IEEE Trans. Ant. and Prop.*, AP-25:104 – 111, 1977.

K. Lamkaouchi, A. Balana, G. Delbos, and W. J. Ellison. Permittivity measurements of lossy liquids in the range 26-110 GHz. *Meas. Sci. Technol.*, 14:444 – 450, 2003.

Q. Liu, F. Weng, and S. J. English. An improved fast microwave water emissivity model. *IEEE Trans. Geosc. Rem. Sens.*, 49(4):1238 – 1250, 2011.

K. Lonitz and A. Geer. New screening of cold-air outbreak regions used in 4D-Var all-sky assimilation. *EUMETSAT/ECMWF Fellowship Programme Research Report*, 35, 2015.

T. Meissner and F. J. Wentz. The complex dielectric constant of pure and sea water from microwave satellite observations. *IEEE Trans. Geosc. Rem. Sens.*, 42(9):1836 – 1849, 2004.

E. Monahan and I. O'Muircheartaigh. Whitecap and the passive remote sensing of the ocean surface. *Int. J. Remote Sens.*, 49:1238 – 1250, 1986.

R. Pottel, U. Kaatze, and V. Uhlendorf. Dielectric reference materials for the high frequency region. *Final report to the B. C. R. project*, 1980.

M. G. M. Richards and R. J. Sheppard. Precision waveguide system in frequency range 29 - 90 ghz. *Meas. Sci. Tech.*, 2:663 – 667, 1991.

A. P. Stogryn, H. T. Bull, K. Ruayi, and S. Iravanchy. The microwave permittivity of sea and fresh water. *Aerojet Internal Report*, 1995.

F. J. Wentz and D. Draper. On-orbit absolute calibration of the global precipitation measurement mcirowave imager. *J. Atmos. Oceanic Technol.*, 33:1393 – 1412, 2016.